

Dalton Transactions

Accepted Manuscript



This is an *Accepted Manuscript*, which has been through the Royal Society of Chemistry peer review process and has been accepted for publication.

Accepted Manuscripts are published online shortly after acceptance, before technical editing, formatting and proof reading. Using this free service, authors can make their results available to the community, in citable form, before we publish the edited article. We will replace this *Accepted Manuscript* with the edited and formatted *Advance Article* as soon as it is available.

You can find more information about *Accepted Manuscripts* in the [Information for Authors](#).

Please note that technical editing may introduce minor changes to the text and/or graphics, which may alter content. The journal's standard [Terms & Conditions](#) and the [Ethical guidelines](#) still apply. In no event shall the Royal Society of Chemistry be held responsible for any errors or omissions in this *Accepted Manuscript* or any consequences arising from the use of any information it contains.

Cite this: DOI: 10.1039/c0xx00000x

www.rsc.org/xxxxxx

ARTICLE TYPE

Forming a ruthenium isomerisation catalyst from Grubbs II: A DFT study

Allan Young^a, Mark A. Vincent^b, Ian H. Hillier^{b*}, Jonathan M. Percy^{a*} and Tell Tuttle^{a*}

Received (in XXX, XXX) Xth XXXXXXXXX 20XX, Accepted Xth XXXXXXXXX 20XX

DOI: 10.1039/b000000x

A DFT investigation into the mechanism for the decomposition of Grubbs 2nd generation pre-catalyst (2) in the presence of methanol, is presented. Gibbs free energy profiles for decomposition of the pre-catalyst (2) via two possible mechanisms were computed. We predict that decomposition following tricyclohexylphosphane dissociation is most favoured compared to direct decomposition of the pre-catalyst (2). However, depending on the reaction conditions, an on-pathway mechanism may be competitive with ruthenium hydride formation.

Introduction

Ruthenium-catalysed alkene metathesis is a highly versatile and widely utilised reaction for forming C=C bonds. The catalysts of Grubbs et al.¹⁻², **1** and **2** (Figure 1), are commonly used to catalyse metathesis reactions.

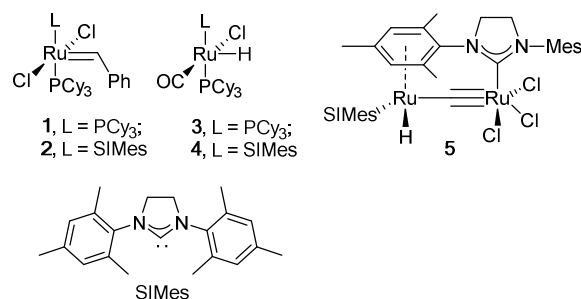


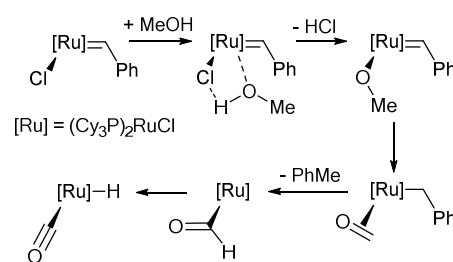
Figure 1. Ruthenium metathesis and isomerisation catalysts.

Work by Dinger and Mol³⁻⁴ has shown that these catalysts can be decomposed in the presence of methanol to produce isomerisation catalysts **3** and **4**. Such isomerisation catalysts have previously caused complications in ring-closing metathesis (RCM) and cross metathesis (CM) reactions, catalysed by Grubbs I and II, by producing unexpected products.⁵ However, conditions now exist which can suppress isomerisation.⁶ Isomerisation can also be exploited in new synthetic strategies.⁷⁻¹⁰ Tandem RCM-isomerisation strategies have also been employed with **2**, where it is used initially as the RCM catalyst and is subsequently activated to form an isomerisation catalyst *in situ*.¹¹⁻¹²

Several ruthenium isomerisation catalysts have been characterized: **4** was prepared initially by Arisawa et al.¹³ and more recently by Beach et al.;¹⁴ diruthenium hydride **5** was characterised by Hong et al.¹⁵ and diphosphine complex **3** was described by Yi and Lee.¹⁶ None of these catalysts had been identified in a metathesis active system (except under forcing conditions),¹⁷ until Ashworth et al.¹⁸ detected **4** by NMR in RCM

and ring opening metathesis polymerisation (ROMP) reactions carried out with very high concentrations of alkene or diene substrates. Hydride complex **4** accumulated throughout the reaction and it was concluded that **4** had not been present in the initial pre-catalyst (**2**) as an impurity.

The most detailed studies of the mechanisms for the formation of **3** and **4** from the corresponding Grubbs pre-catalysts were carried out by Dinger and Mol; Scheme 1 summarises their outline mechanism.⁴

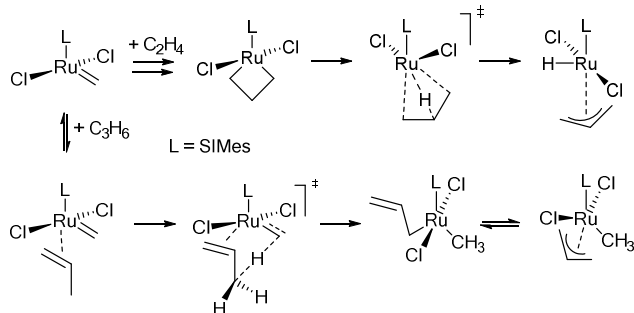


Scheme 1

Work on the conversion of **1** to **3** in the presence of methanol, showed that the hydride is produced by dehydrogenation of the alcohol. This process has previously been shown to provide aldehydes, which further react with the ruthenium to provide the carbonyl and hydride moieties.¹⁹ The origin of the hydride was confirmed by a deuterium labelling study.³ Dinger and Mol proposed a mechanism for the conversion of **1** to **3** (see Scheme 1); they also proposed that this mechanism could be extended to the decomposition of the second-generation catalyst **2** to **4**. While the mechanisms appear reasonable and precedented, they have not been studied using current computational methodology; their energetic costs therefore remain unknown, which makes their kinetic competence inestimable.

While isomerisation is most often attributed to the action of species like **3** and **4**, alternative pathways have been proposed, based on the second generation pre-catalysts. Van Rensburg and co-workers investigated a mechanism which involved hydride

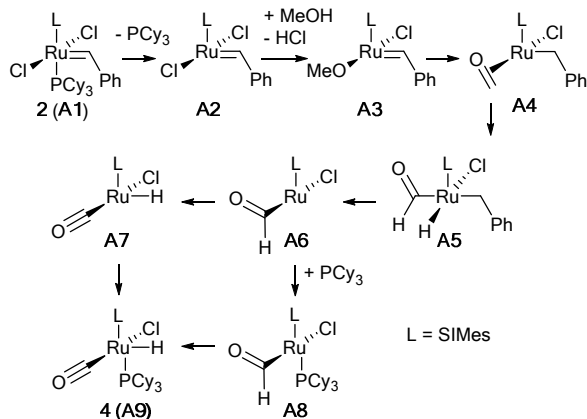
transfer from carbon to ruthenium within a metallocyclobutane, an on-pathway intermediate formed from the reaction between an alkene (ethene is used to illustrate this in Scheme 2, pathway a) and an Ru methylidene complex.²⁰ Reorganisation via (η^3 -allyl)ruthenium hydride species **6** provides an isomerisation pathway. Nolan and co-workers²¹ proposed an alternative on-pathway mechanism (Scheme 2, pathway b); coordination of an alkene to an Ru methylidene (propene is used to illustrate this), followed by hydride transfer to the Ru alkylidene to form a range of interconverting σ -allyl and η^3 -allyl species **7a** and **7b**.



Scheme 2

Relocation of an hydrogen atom then regenerates a 14e alkyldiene catalyst. We investigated these pathways computationally,¹⁸ finding that isomerisation via **4** was facile compared to the on-pathway mechanisms. Of these, the sequence based on van Rensburg's work (pathway a) was energetically easier. However, our work was unable to take account of the energetic cost of the formation of the active catalyst derived from **2**. A more complete picture would emerge if the degree of difficulty of formation of pre-catalysts **3** and **4** was known.

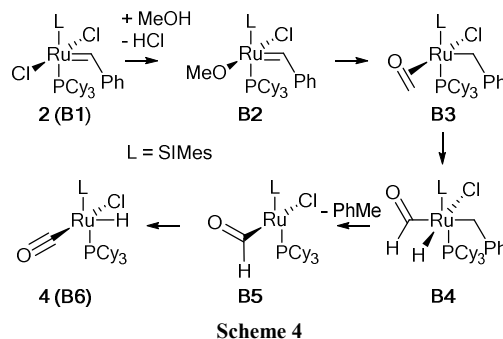
Here we use computational methods to study the decomposition of the widely-used Grubbs second-generation pre-catalyst **2** in the presence of methanol via two possible mechanisms. The first mechanism, referred to as phosphine-off (see Scheme 3), begins with dissociation of the tricyclohexylphosphane ligand to form alkyldiene **A2**.



Scheme 3

This dissociation event (initiation) is the first step in alkene metathesis reactions.²² It is kinetically significant, controlling the amount of catalytically-active species present in the metathesis rate, though there does not appear to be a simple relationship

between its rate and that of subsequent isomerisation reactions.²³ This step differentiates the two mechanisms being studied; the second mechanism, referred to as phosphine-on (see Scheme 4) and which is associative,²⁴ follows decomposition with the phosphine ligand bound throughout (vide infra). This pathway avoids the energetic cost of initiation and has a distinct kinetic advantage; **2** (**A1**) will be present in significantly higher concentration²⁵ than **A2** so the rate of reaction would be much higher, even if the second-order rate constant is relatively small.



Scheme 4

4.5 Computational Methods

Density functional theory (DFT) was used for the geometry optimisations of all reactants, transition structures (TSs), intermediates and products. In all calculations, the ruthenium atom was described by the MWB28²⁶ effective core potential and corresponding basis set, while the 6-31G(d,p) basis set was used for all other atoms. All geometry optimisations were performed in Gaussian09,²⁷ with the M06L functional²⁸ which has been shown to be effective for similar ruthenium-based compounds.²⁹⁻³¹ The optimised geometries were characterised as minima or transition structures by performing harmonic frequency calculations, which also enabled calculation of the zero-point energies (ZPE), enthalpies (H), entropies (S) and Gibbs free energies (G) at 298K.

In order to determine whether the inclusion of solvent via a polarisable continuum model would affect the calculated energetics of the reaction mechanisms, the structures of the methylene analogs (*vide infra*) were reoptimised in the solvent phase using the CPCM solvation method as implemented in G09, with dichloromethane ($\epsilon=8.9$) as the solvent. The inclusion of solvent via the polarisable continuum model does not significantly affect the calculated energetics for the reaction pathway (Figure S2, Supporting Information). Therefore, the energetics for the larger systems were calculated in the gas phase.

Results and Discussion

7.0 Phosphine-off pathway. Figure 2 represents the phosphine-off pathway. The initial step of phosphine ligand dissociation (**A1**→**A2**) is endergonic ($\Delta G = 15.6$ kcal/mol, see); however this reaction is kinetically competent for this compound at room temperature.²² The subsequent forward barrier (**TSA2**→**A3**, Figure 3) of 20.4 kcal/mol is achievable, although since the reverse barrier to **A2** is only 5 kcal/mol it is likely that only a very small quantity of **A3** would be formed. Metathesis reactions are rarely carried out in sealed systems, so it is likely that the HCl

generated in this step could be evolved from the reaction mixture or ionized by methanol, effectively re-setting the energy of **A3** to zero and preventing the reverse reaction from occurring.

The barrier for **A3**→**A4** is 25.2 kcal/mol, which would be achievable when taken in the context of a room temperature reaction, although the quantity of **A4** formed would be small.

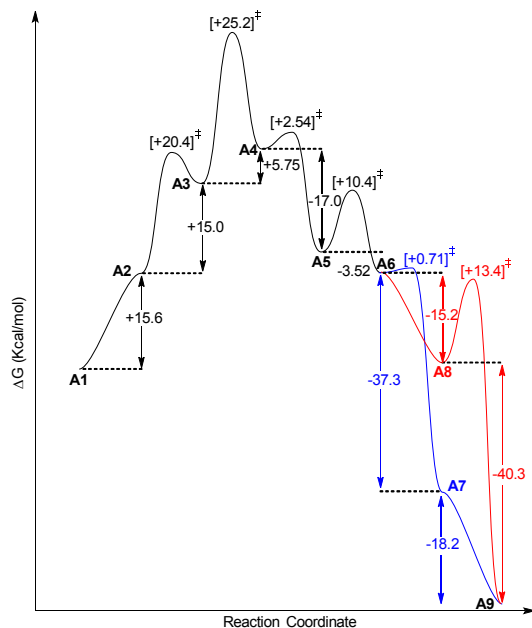


Figure 2. Gibbs free energy profile for phosphine-off mechanism.

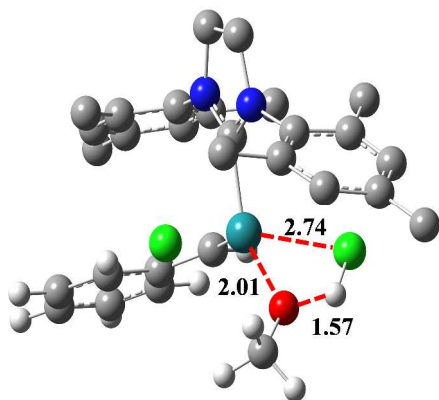


Figure 3. Optimised geometry of **TSA2**→**A3**. Hydrogen atoms are omitted from the SIMes ligand for clarity, and distances are in Angstroms.

We note that for this step that involves H^- , methoxide is a well-known hydride transfer agent and that the LUMO of **A3** has its largest atomic contributions on the hydride-accepting alkyldiene carbon (see Figure S1)). After these initial barriers, the next barrier (**A4**→**A5**) is low (2.54 kcal/mol) and the lower free energy of the next intermediate would drive this step ($\Delta G = -17$ kcal/mol). Step **A5**→**A6** delivers a $12e^-$ species, which at first seems unreasonable. However, it faces a forward barrier of only 0.71 kcal/mol and would thus be an unstable intermediate, which would convert to the hydrido carbonyl species **A7** as soon as it

was formed. The barrier for this step is low due to the CHO ligand being in the equatorial plane, with the hydrogen well positioned for abstraction by the ruthenium (see Figure 4).

The mechanism via species **A7** is more energetically favourable than via **A8**, since the barrier to the hydride species is lower (**A6**→**A7** = 0.7 kcal/mol whereas **A8**→**A9** = 13.4 kcal/mol). This is due to the impact of the tricyclohexylphosphane ligand which restricts the movement of the ligand and forces it out of the optimum alignment achieved for **TSA6**→**A7**. Therefore, it can be assumed that the mechanism proceeds via **A7** and the next step would be association of the tricyclohexylphosphane, which is favourable ($\Delta G = -18.2$ kcal/mol).

The computed free energy profile (see Figure 2) would support the work of Ashworth et al.¹⁸ which showed that only a small amount of the active isomerisation pre-catalyst **4** formed. Due to the barrier associated with **A3**→**A4** ($\Delta G = 25.2$ kcal/mol) it is unlikely that a large amount of intermediate **A4** would be formed, so only a small amount of the final product, **4(A9)**, would be formed in turn.

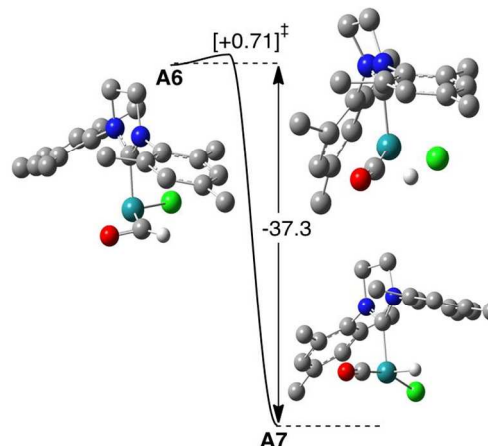


Figure 4. Optimised geometry and relative free energies (kcal mol^{-1}) of **A6**, **TSA6**→**A7** and **A7**.

Another mechanism, the direct formation of **A4** from **A2** was also investigated. However, a transition structure for this step could not be identified so that an alternative was investigated. As opposed to transferring hydrogen to the alkyldiene carbon, the hydrogen was now transferred onto the ruthenium. A transition structure for this was identified with an associated ΔG of 53.2 kcal/mol, a value showing that this would not be competitive with the initial mechanism.

A further mechanism investigated was to deprotonate the methanol molecule using the outgoing tricyclohexylphosphane ligand, leaving behind a methoxide to occupy the vacated axial coordination site (see Scheme 2). A transition structure for this reaction could not be identified; however the free energy difference between the reactants and products is 90.8 kcal/mol, which would therefore not be competitive with the initial mechanism.

Phosphine-on pathway. The competence of a pathway which does not require phosphine dissociation is of considerable interest because the pre-catalyst itself rather than **A2** would then be

present in the rate equation for the formation of **A7**. As **A2** is the product of a strongly unfavourable equilibrium, its concentration is likely to be very low. The initial step (**B1**→**B2**) of this mechanism corresponds to the second step of the phosphine-off mechanism (**A2**→**A3**). However, the barrier for this mechanism is larger at 54.6 kcal/mol (see Figure 5), which can be rationalised by studying the optimised geometry of the transition structure (see Figure 6). This shows that the steric environment for a molecule of methanol to approach is restricted. This increased barrier would be difficult to surmount at room temperature, ruling out this mechanism as responsible for the conversion of **2** to **4**.

The following barrier (**B2**→**B3**) is also higher than the corresponding barrier in the phosphine-off mechanism (**A3**→**A4**), 30.1 kcal/mol compared with 25.2 kcal/mol respectively. This is less of an increase than occurs with the previous step; the steric effects are much smaller because the reaction is intramolecular. The third barrier (**B3**→**B4**) is again higher than the comparable phosphine-off step (**A4**→**A5**), at 9.2 kcal/mol compared with 2.5 kcal/mol.

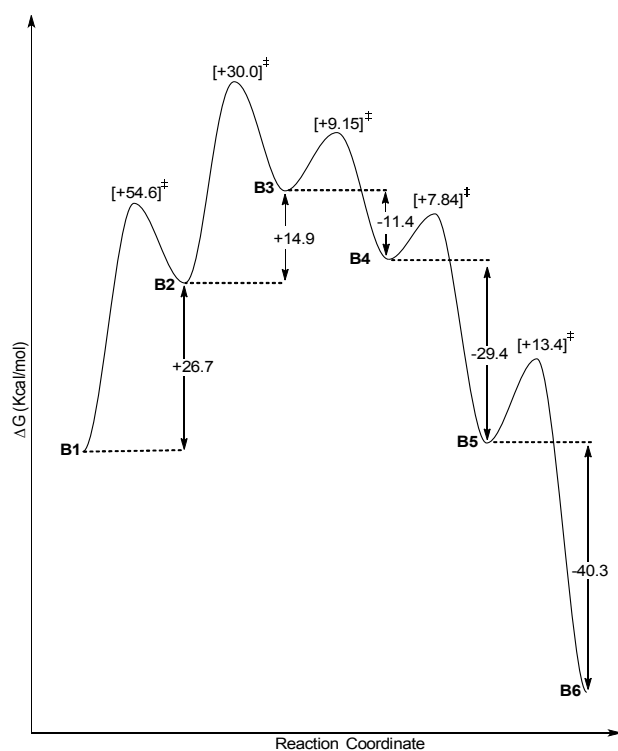


Figure 5. Gibbs free energy profile for phosphine-on mechanism.

The fourth barrier in this mechanism is 7.8 kcal/mol, which is lower than the corresponding step in the phosphine-off mechanism (**A5**→**A6**), due to steric strain relief when the toluene dissociates (decreasing the number of ligands around the metal). Both the final step **B4**→**B5**, and **A8**→**A9** of the phosphine-off mechanism, have a barrier of 13.4 kcal/mol, which is higher than the barrier of 0.71 kcal/mol for the corresponding hydrogen abstraction (**A6**→**A7**) in the phosphine-off mechanism. The difference is due to the steric influence of the tricyclohexylphosphane ligand restricting this reaction to the equatorial plane. The calculation of the barriers for **C2** → **C5** (from methylidene) allows a direct comparison of the relative

costs of the isomerisation catalysed by **A7** and the van Rensburg mechanism (Figure 7) (for a direct comparison with the previously calculated pathway, all structures along the **C2** → **C5** pathway were also optimised using the CPCM solvent model as described in the Supporting Information).

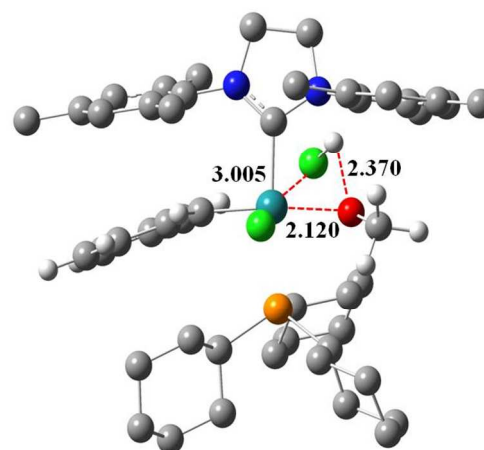


Figure 6. Optimised geometry of **TS****B1**→**B2**, Note hydrogens omitted from the SIMes and **PCy**₃ ligand for clarity, and distances in Angstroms

Free energy differences and barrier heights were similar to those calculated for benzylidene **A2**, with the formation of the methoxide complex strongly endergonic (+18.6 kcal/mol, Figure 7), followed by a moderately high barrier to hydride transfer (+21.6 kcal/mol, relative to **C3**, Figure 7). The formation of **A7** is very strongly thermodynamically favourable overall; this is due to the formation of the hydride species and the release of ethane from **C5** (in analogy to the formation of the hydride and release of toluene along the **A5** → **A7** pathway, $\Delta G = -40.8$ kcal/mol, Figure 2). Nonetheless, the on-pathway mechanism proposed by van Rensburg (red line, Figure 7) looks more competitive when compared with the initial stages of the phosphine-off pathway for methylidene (blue line, Figure 7).

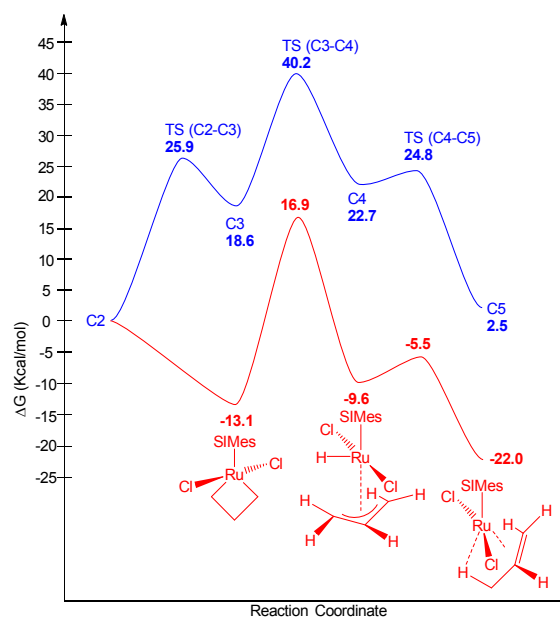


Figure 7. Relative Gibbs free energies of methyldiene phosphine-off (blue) and van Rensburg on-pathway (red) for ruthenium hydride generation.

The van Rensburg mechanism begins with a strongly favourable event (metallocyclobutane formation), followed by a maximum barrier of 30.0 kcal/mol (Figure 7). The reaction is exergonic. We calculated the energetics of the van Rensburg pathway from methyldiene and ethene, but substrate diene can take the place of ethene; metallocyclobutanation reactions of ethene and terminal alkenes have similar barriers and energetics, and the total alkene concentration is considerably higher than that of adventitious alcohol.

Conclusions

Two mechanisms for the decomposition of **2** in the presence of methanol to produce **4** were studied. The phosphine-off

mechanism provides the most favourable route to the ruthenium isomerisation catalyst **4**. This mechanism is more favourable than the phosphine-on mechanism due to the higher transition state barriers encountered at the beginning of the phosphine-on mechanism. The initial two barriers in the phosphine-off mechanism provide an explanation for the experimentally observed (and very low) quantity of **4** observed by Ashworth et al.¹⁸ For the scenario described by Dinger and Mol, the high concentration of alcohol will favour the conversion of **A2** (or **C2**) to **A7** (or **C7**). However, under synthetic metathesis conditions, the on-pathway mechanism proposed by van Rensburg and co-workers now looks considerably more competitive and must be considered seriously as an explanation for alkene isomerisation under synthetic metathesis conditions when efforts have been made to ensure that reaction solvents are free from alcohol contaminants.

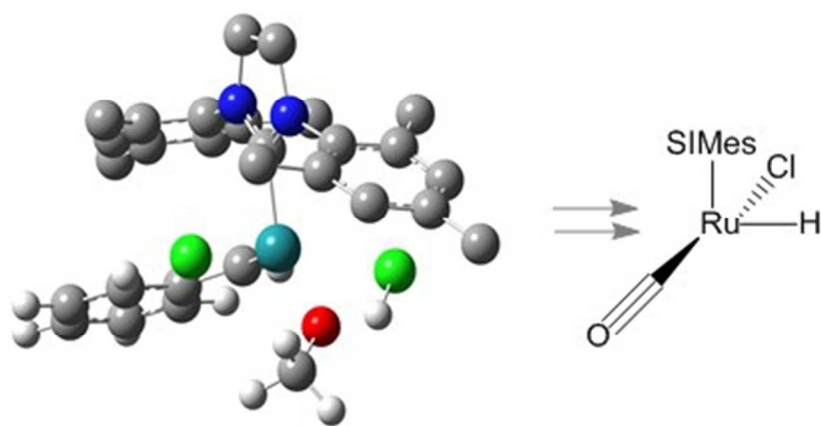
Notes and references

^a WestCHEM Department of Pure & Applied Chemistry, University of Strathclyde, 295 Cathedral Street, Glasgow, G1 1XL, UK. Tel: +44 (0)141 548 4398; E-mail: jonathan.percy@strath.ac.uk; tell.tuttle@strath.ac.uk

^b School of Chemistry, University of Manchester, Manchester M13 9PL UK Tel (0)1612754687, E-mail: ian.hillier@manchester.ac.uk

[†] Electronic Supplementary Information (ESI) available: LUMO of **A3**; cartesian coordinates; and energies of **A1-C5**. See DOI: 10.1039/b000000x/

- M. Scholl, S. Ding, C. W. Lee and R. H. Grubbs, *Org. Lett.*, 1999, **1**, 953-956.
- P. Schwab, R. H. Grubbs and J. W. Ziller, *J. Am. Chem. Soc.*, 1996, **118**, 100-110.
- M. B. Dinger and J. C. Mol, *Eur. J. Inorg. Chem.*, 2003, 2827-2833.
- M. B. Dinger and J. C. Mol, *Organometallics*, 2003, **22**, 5291-5296.
- J. S. Clark, *Chem. Commun.*, 2006, 3571-3581.
- J. R. Clark and S. T. Diver, *Org. Lett.*, 2011, **13**, 2896-2899.
- W. A. L. van Otterlo, G. L. Morgans, S. D. Khanye, B. A. A. Aderibigbe, J. P. Michael and D. G. Billing, *Tetrahedron Lett.*, 2004, **45**, 9171-9175.
- T. J. Donohoe, T. J. C. O'Riordan and C. P. Rosa, *Angew. Chem., Int. Ed.*, 2009, **48**, 1014-1017.
- G. De Bo and I. E. Marko, *Eur. J. Org. Chem.*, 2011, 1859-1869.
- D. B. Yadav, G. L. Morgans, B. A. Aderibigbe, L. G. Madeley, M. A. Fernandes, J. P. Michael, C. B. de Koning and W. A. L. van Otterlo, *Tetrahedron*, 2011, **67**, 2991-2997.
- B. Schmidt and O. Kunz, *Synlett*, 2012, 851-854.
- A. E. Sutton, B. A. Seigal, D. F. Finnegan and M. L. Snapper, *J. Am. Chem. Soc.*, 2002, **124**, 13390-13391.
- M. Arisawa, Y. Terada, K. Takahashi, M. Nakagawa and A. Nishida, *J. Org. Chem.*, 2006, **71**, 4255-4261.
- N. J. Beach, U. L. Dharmasena, S. D. Drouin and D. E. Fogg, *Adv. Synth. Catal.*, 2008, **350**, 773-777.
- S. H. Hong, A. G. Wenzel, T. T. Salguero, M. W. Day and R. H. Grubbs, *J. Am. Chem. Soc.*, 2007, **129**, 7961-7968.
- C. S. Yi and D. W. Lee, *Organometallics*, 1999, **18**, 5152-5156.
- B. Schmidt, *J. Mol. Catal. A: Chem.*, 2006, 254, 53-57.
- I. W. Ashworth, I. H. Hillier, D. J. Nelson, J. M. Percy and M. A. Vincent, *Eur. J. Org. Chem.*, 2012, 5673-5677.
- Y. Z. Chen, W. C. Chan, C. P. Lau, H. S. Chu, H. L. Lee and G. C. Jia, *Organometallics*, 1997, **16**, 1241-1246.
- W. J. van Rensburg, P. J. Steynberg, W. H. Meyer, M. M. Kirk and G. S. Forman, *J. Am. Chem. Soc.*, 2004, **126**, 14332-14333.
- D. Bourgeois, A. Pancrazi, S. P. Nolan and J. Prunet, *J. Organomet. Chem.*, 2002, **643**, 247-252.
- E. L. Dias, S. T. Nguyen and R. H. Grubbs, *J. Am. Chem. Soc.*, 1997, **119**, 3887-3897.
- D. J. Nelson and J. M. Percy, *Dalton Trans.*, 2014, **43**, 4674 - 4679.
- I. W. Ashworth, I. H. Hillier, D. J. Nelson, J. M. Percy and M. A. Vincent, *ACS Catalysis*, 2013, **3**, 1929-1939.
- D. J. Nelson, D. Carboni, I. W. Ashworth and J. M. Percy, *J. Org. Chem.*, 2011, **76**, 8386-8393.
- D. Andrae, U. Häußermann, M. Dolg, H. Stoll and H. Preuß, *Theoret. Chim. Acta*, 1990, **77**, 123-141.
- M. J. Frisch, G. W. Trucks, H. B. Schlegel, G. E. Scuseria, M. A. Robb, J. R. Cheeseman, G. Scalmani, V. Barone, B. Mennucci, G. A. Petersson, H. Nakatsuji, M. Caricato, X. Li, H. P. Hratchian, A. F. Izmaylov, J. Bloino, G. Zheng, J. L. Sonnenberg, M. Hada, M. Ehara, K. Toyota, R. Fukuda, J. Hasegawa, M. Ishida, T. Nakajima, Y. Honda, O. Kitao, H. Nakai, T. Vreven, J. J. A. Montgomery, J. E. Peralta, F. Ogliaro, M. Bearpark, J. J. Heyd, E. Brothers, K. N. Kudin, V. N. Staroverov, R. Kobayashi, J. Normand, K. Raghavachari, A. Rendell, J. C. Burant, S. S. Iyengar, J. Tomasi, M. Cossi, N. Rega, J. M. Millam, M. Klene, J. E. Knox, J. B. Cross, V. Bakken, C. Adamo, J. Jaramillo, R. Gomperts, R. E. Stratmann, O. Yazyev, A. J. Austin, R. Cammi, C. Pomelli, J. W. Ochterski, R. L. Martin, K. Morokuma, V. G. Zakrzewski, G. A. Voth, P. Salvador, J. J. Dannenberg, S. Dapprich, A. D. Daniels, O. Farkas, J. B. Foresman, J. V. Ortiz, J. Cioslowski and D. J. Fox, Gaussian, Inc., Wallingford CT, 2009.
- Y. Zhao and D. G. Truhlar, *J. Chem. Phys.*, 2006, **124**, 224105/1-6.
- Y. Zhao and D. G. Truhlar, *Acc. Chem. Res.*, 2008, **41**, 157-167.
- Y. Zhao and D. G. Truhlar, *J. Chem. Theory Comput.*, 2009, **5**, 324-333.
- S. Pandian, I. H. Hillier, M. A. Vincent, N. A. Burton, I. W. Ashworth, D. J. Nelson, J. M. Percy and G. Rinaudo, *Chem. Phys. Lett.*, 2009, **476**, 37-40.



A pathway for methanolysis of Grubbs' second generation catalyst has been computed.
111x62mm (96 x 96 DPI)